Examining the Adsorption (Vapor−Liquid Equilibria) of Short-Chain Hydrocarbons in Low-Density Polyethylene with the SAFT-VR Approach

Clare McCabe,*,†,‡ Amparo Galindo,§ M. Nieves García-Lisbona,§ and George Jackson§

Department of Chemical Engineering, University of Tennessee, Knoxville, Tennessee 37996-2200, and Department of Chemical Engineering and Chemical Technology, Imperial College of Science, Technology and Medicine, Prince Consort Road, London SW7 2BY, U.K.

The versatility of the SAFT-VR approach in the prediction of fluid-phase equilibria of complex fluids is illustrated for systems of short and long hydrocarbons. In particular, we examine the vapor−liquid equilibrium of a mixture of methane + hexatriacontane ($C_{36}H_{74}$) and the adsorption and coadsorption of light alkanes on low-density polyethylene. The molecules are modeled as chains of square-well segments, and the approach incorporates separate contributions to take into account the effect of monomer−monomer interactions and the bonding of the segments to form chains. In previous work (McCabe, C.; Jackson, G. *Phys. Chem. Chem. Phys.* **1999**, *1*, 2057), the phase behavior of pure long-chain *n*-alkane molecules was examined using the SAFT-VR approach; the intermolecular potential parameters were found to tend to a limiting value as the chain length of the *n*-alkane increases. Linear relationships with molecular weight for these parameters are used to model the polyethylene polymer in this work.

Introduction

The phase behavior and thermodynamics of hydrocarbon fluids are central to the petrochemical industry in the general context of oil recovery and in the subsequent production of waxes and polymers, which find widespread use. In particular, a knowledge of the phase behavior of mixtures of small and large hydrocarbons is crucial to the design and optimization of polymer production and processing. The equilibrium compositions of the reacting components determine the outcome of the polymerization reaction, and in downstream separation processes, the polymer product needs to be separated from unreacted monomers, solvents, and additives. To obtain a final product with the right properties, it is also important to ensure that the mixture remains in one phase during the polymerization process. Experimental studies under reactor conditions are, however, expensive to run, with safety considerations adding to the cost. In this context, predictive theoretical methods are particularly useful.

Mixtures of solvents and polymers (and of short and long hydrocarbons) generally exhibit a fluid-phase behavior of type IV or V in the scheme of Scott and van Konynenburg.[1] Their phase diagrams are characterized by a discontinuous vapor−liquid critical line, reflecting a phase separation of two dense fluids, one polymer-rich and another solvent-rich, usually in the high-pressure regime; as the temperature is lowered at a fixed pressure, the two phases become miscible at a lower critical solution temperature (LCST). Type IV systems exhibit an additional liquid−liquid immiscibility and upper critical solution temperature (UCST) in the low-temperature region of the phase diagram. In most cases, however, solid phases pre-empt this liquid−liquid immiscibility, and only type V phase behavior is observed. For the largest differences in size between the two components, e.g. for a mixture of methane and hexatriacontane ($C_{36}H_{74}$), type III phase behavior is observed. Type III phase diagrams are characterized by a large region of liquid−liquid immiscibility, with the locus of UCSTs being found at relatively high temperatures, merging into the vapor−liquid critical line. LCSTs are not found in these systems, but instead, a critical line runs continuously from the critical point of the less volatile component (the polymer) to the locus of the UCSTs. A second small branch of the vapor−liquid critical curve runs from the critical point of the more volatile component (the small hydrocarbon) to the end of the three-phase line. This having been said, we shall not be concerned with critical lines here but rather will focus on the gas−liquid equilibrium in the system, which is of importance in the flash separation step of the polymer production process.

Reliable experimental data are readily available for the thermodynamic and phase equilibrium properties of light (small) hydrocarbons (molecular weight < 500),[2−4] but those for heavier hydrocarbons are more scarce. Experimental vapor pressures and saturated liquid densities of *n*-alkanes up to and including hexatriacontane ($C_{36}H_{74}$) have been determined,[5,6] although thermal instability makes accurate experimental measurement extremely difficult for chains longer than decane.[7] As one might expect, experimental fluid-phase

* Corresponding author: clare@utk.edu.

† University of Tennessee

‡ Permanent address from January 1, 2002: Department of Chemical Engineering, Colorado School of Mines, Golden, CO 80401.

§ Imperial College of Science, Technology and Medicine

10.1021/ie0101386 CCC: $20.00
Published on Web 00/00/0000

equilibrium data for polymer systems is even more limited, especially at high pressures. Furthermore, typical polymer products are not true pure fluids, but polydispersed mixtures of molecules of varying chain length and degree of branching. The development of an accurate theoretical framework for interpreting and ultimately predicting the thermodynamic properties and phase behavior of polymer systems is hence becoming increasingly important.[8]

At present, thermodynamic models for polymer solutions fall into two broad categories: activity coefficient models[9−11] (e.g., the Flory−Huggins theory,[12] polymer NRTL,[13] and polymer UNIFAC or UNIFAC-FV[14]), and equations of state (e.g., Sanchez−Lacombe,[15−17] cubic equations of state such as polymer-SRK,[18] and SAFT[19,20]). The classic lattice model of Flory and Huggins is still one of the most popular because of its simplicity. In the original approach all lattice sites are occupied, and so the mixture is incompressible. Sanchez and Lacombe[15−17] developed a very similar model, with the important difference of allowing for empty lattice sites, in this way bringing in a density and pressure dependence. These models are better suited for studies of systems at liquidlike densities because they are based on a lattice. Cubic equations of state, such as the Soave−Redlich−Kwong (SRK) equation, combined with the Flory−Huggins activity coefficient model have been proposed to overcome this difficulty.[21,22] However, the most promising models in terms of predictive capabilities are those derived from thermodynamic perturbation theory. These approaches are applicable over a wide range of densities, from gas to liquid, and for small and large molecules. In particular, the statistical associating fluid theory[19,20] (SAFT) was specifically developed to study chain and associating chain fluids.

The SAFT approach stems from the perturbation theory of Wertheim.[23−26] It was originally developed in the late 1980s by Chapman and co-workers[19,20] to model associating fluids as chains of Lennard-Jones segments with associating sites. In the equation, separate contributions are incorporated to take into account segment−segment interactions, segment bonding to form chains, association, and dispersion interactions. As SAFT explicitly takes into account molecular nonsphericity, it provides a powerful method for studying the phase behavior of chain molecules. Huang and Radosz[27−30] have successfully correlated the equilibrium data of a vast range of pure substances and mixtures, including polymer fluids, using a version of the SAFT approach with a modified attractive term. In the original approach, and in that of Huang and Radosz, a fluid of hard-sphere monomers is taken as the reference system. More recently, a number of modifications have been proposed that incorporate a more accurate description of the reference Lennard-Jones monomer fluid.[31−41] These approaches have been used to study alkane and polymer-like fluids, and comparisons have been made with experimental and computer simulation data.

The simplest version of the SAFT approach describes chains of associating hard-sphere (HS) segments with the dispersion interactions described at the van der Waals mean-field level (SAFT-HS).[42,43] This approach is especially suited to studies of strongly associating systems, where the association dominates the attractive contribution and the dispersion forces can be adequately described by a mean-field interaction. For example, the critical behavior of *n*-alkanes,[69] the high-pressure critical lines of mixtures of water + alkanes,[45] mixtures containing hydrogen fluoride,[44] and water + polyoxyethylene surfactant mixtures[46,47] have been modeled with SAFT-HS.

The SAFT approach has been generalized to describe chain molecules of attractive monomer segments incorporating attractive potentials of variable range (SAFT-VR[48,49]). In this case, the long-range dispersion interactions are treated via a high-temperature perturbation expansion up to second order. An additional parameter λ, which characterizes the range of the attractive part of the potential, is used, resulting in a significant improvement over the treatment used in the SAFT-HS approach. In terms of the chain and association contributions, the contact distribution function of the fluid of attractive monomers is used instead of that of the hard-sphere system. Radosz and Adidharma[50,51] presented a similar approach (termed SAFT1) for chains of square-well segments adding a term to correct for the truncation of the high-temperature expansion at second order. Using this approach they studied a number of alkane + polymer fluids finding good agreement with experimental data.[52−54]

In previous work, we have used the SAFT-VR approach extensively to describe the fluid-phase behavior of a wide range of industrially important substances and their mixtures (see, for example, refs 55−61). In particular, we have examined the fluid-phase equilibria of the *n*-alkanes and their binary mixtures.[48,55,56,58] Short *n*-alkane chains were studied initially, and the change in phase behavior from type I to type V (according to the classification of Scott and van Konynenburg[1]) as the molecular weight of one component is increased was illustrated.[56] In a comprehensive study, *n*-alkanes from *n*-nonane (C_9H_{20}) to *n*-hexatriacontane ($C_{36}H_{74}$) were examined, and simple linear relationships with molecular weight were obtained for the intermolecular potential parameters.[58] Similar prescriptions for the parameters of hydrocarbons have been proposed by Fu and Sandler[62] for the simplified SAFT equation and Blas and Vega[63] for the soft-SAFT approach. These relations allow for the determination of the potential model parameters of the longer members of the *n*-alkane homologous series for which no experimental data are available. The accuracy of this method was confirmed by comparing the SAFT-VR predictions for the saturated liquid density of octatetracontane ($C_{48}H_{98}$) with pseudo-experimental data from the Gibbs ensemble computer simulations of Smit et al;[64,65] given the excellent agreement obtained between the SAFT-VR prediction and the simulation, we extend the approach to study polymeric systems. In particular, we examined the vapor−liquid phase behavior of short-chain *n*-alkane + low-density polyethylene (LDPE) mixtures. The aim of this paper is to show that, by using the linear relations obtained from the intermolecular potential parameters of the alkanes,[58] we can easily determine suitable parameters to model the vapor−liquid phase behavior of polymer systems.

The SAFT-VR Approach

In the SAFT approach, the free energy of a mixture of associating chain molecules can be written as the sum of four separate contributions

$$\frac{A}{NkT} = \frac{A^{\mathrm{IDEAL}}}{NkT} + \frac{A^{\mathrm{MONO}}}{NkT} + \frac{A^{\mathrm{CHAIN}}}{NkT} + \frac{A^{\mathrm{ASSOC}}}{NkT}$$

where N is the number of molecules, k is the Boltzmann constant, and T is the temperature. A^{IDEAL} is the ideal free energy, A^{MONO} is the contribution to the free energy due to the monomeric segments, A^{CHAIN} is the contribution due to the formation of a chain of m monomers, and A^{ASSOC} is the contribution due to association. In this work, we do not consider the association term because we are dealing with nonassociating systems. In the SAFT-VR[48,49] approach, the monomer segments are modeled with an arbitrary attractive potential of variable range λ and depth ϵ

$$u(r) = u^{HS}(r;\sigma) - \epsilon\phi(r;\lambda)$$

In the case of square-well monomers, the intermolecular potential is given by

$$u(r) = \begin{cases} +\infty & \text{if } r < \sigma \\ -\epsilon & \text{if } \sigma \le r < \lambda\sigma \\ 0 & \text{if } r \ge \lambda\sigma \end{cases}$$

where r is the distance and σ defines the contact distance between the spherical segments. The monomer free energy is then written as a second-order high-temperature perturbation expansion[66]

$$\frac{A^{MONO}}{NkT} = \frac{A^{HS}}{NkT} + \frac{1}{kTNkT}A_1 + \frac{1}{(kT)^2NkT}A_2$$

where A^{HS} is the free energy of the reference hard-sphere fluid given by Boublik[67] and Mansoori et al.[68] A_1 is the mean attractive attractive energy, and A_2 describes the energy fluctuations (see refs 48 and 49 for more details).

As in other versions of the SAFT approach, the free-energy contribution due to chain formation is given by the number of contacts in the chain ($m - 1$) and the contact-pair distribution function of the reference monomer fluid, $g^{MONO}(\sigma)$, which, for a pure fluid, is given by

$$\frac{A^{CHAIN}}{NkT} = -(m-1)\ln g^{MONO}(\sigma)$$

In the SAFT-VR approach, $g^{MONO}(\sigma)$ is written as a first-order perturbation expansion

$$g^{MONO}(\sigma) = g^{HS}(\sigma) + \frac{1}{kT}g_1(\sigma)$$

where $g^{HS}(\sigma)$ is the hard-sphere radial distribution function. A closed form for $g_1(\sigma)$ can be obtained from the pressure expression (the Clausius virial theorem) and the first derivative of the free energy with respect to the density (see ref 48). The pressure and chemical potential needed to evaluate phase equilibria are obtained from the free energy using the standard thermodynamic relations. Phase equilibria between phases I and II in mixtures requires that the temperature, pressure, and chemical potential of each component in each phase be equal, although in this work, we do not allow the polymer into the gas phase. Hence, the condition becomes

$$T^I = T^{II},\ p^I = p^{II},\ y_2 = 0,\ \mu_1^I = \mu_1^{II}$$

Table 1. SAFT-VR Potential Model Parameters[a]

molecule	M_w (g mol^{-1})	m	λ	σ (Å)	ϵ/k (K)
CH_4	16	1.00	1.444	3.670	168.8
C_2H_4	28	1.20	1.445	3.743	236.1
C_4H_{10}	58	2.00	1.501	3.887	256.3
C_5H_{12}	72	2.33	1.505	3.931	265.0
$C_{36}H_{74}$	506	12.67	1.565	4.037	286.8
LDPE	76 000	1810	1.614	4.026	264.8
LDPE	248 700	5921	1.614	4.026	264.8

[a] M_w is the molecular weight of the molecule, m is the number of spherical segments in the model, λ is the square-well range, σ *is* the diameter of each segment, and ϵ is the square-well depth.

where y is the mole fraction in the gas phase and the subscripts 1 and 2 denote the short-chain and polymer components of the mixture, respectively.

Intermolecular Potential Parameters and Results

The alkane molecules are modeled as homonuclear chains formed from m tangent square-well segments of hard-core diameter σ. A simple empirical relationship developed in earlier work[45,69] is used to determine the number of spherical segments m from the number of carbon atoms C: $m = {}^1/_3(C - 1) + 1$. For polymer molecules, the number of carbon atoms is obtained from the average molecular weight. In general, pure-component parameters in the SAFT-VR approach (σ, ϵ, and λ) are obtained by fitting to experimental vapor pressure and saturated liquid density data from the triple point to the critical point using a simplex method.[70] The parameters are combined to give an expression for the integrated van der Waals attractive energy α; in the case of a square-well potential, the relation is given by $\alpha = 2\pi\epsilon\sigma^3(\lambda^3 - 1)/3$.[48] These parameters have been determined in previous work for n-alkanes from methane to n-hexatriacontane ($C_{36}H_{74}$).[58] Simple linear relations[58] can be used for the longer n-alkanes for which limited experimental data is available

$$m\lambda = 0.039\ 00M_w + 0.8730$$

$$m\sigma^3 = 1.566M_w + 24.02$$

$$m(\epsilon/k) = 6.343M_w + 76.38$$

where M_w is the molecular weight of the chain molecule. Using these relations, the parameters of any polyethylene polymer can be determined from its molecular weight. As expected, the parameters tend to limiting values as the molecular weight and chain length of the molecules increase. Average limiting values of the parameters are used for all of the polyethylene polymers; the different polymers are characterized in terms of their size with the chain-length parameter m (see Table 1 for details). To study the fluid-phase behavior of the mixtures, the unlike parameters σ_{ij}, ϵ_{ij}, and λ_{ij} need to be determined. In this work, the unlike size and energy parameters are determined using the Lorentz−Berthelot combining rules,[49,71] and the unlike range parameter is determined from the arithmetic mean

$$\lambda_{ij} = \frac{\sigma_{ii}\lambda_{ii} + \sigma_{jj}\lambda_{jj}}{\sigma_{ii} + \sigma_{jj}}$$

This corresponds to the MX3b mixing rule of ref 49. We find that there is no need to readjust the unlike

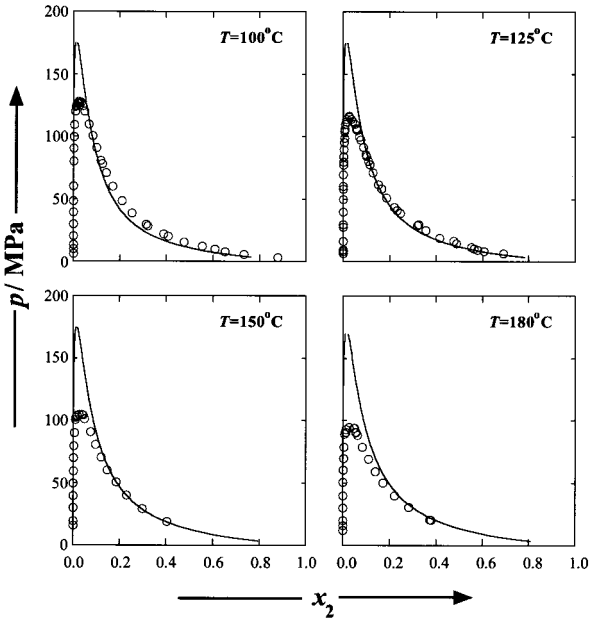

Figure 1. Constant-temperature *px* slices of the phase diagram for methane (1) + *n*-hexatriacontane ($C_{36}H_{74}$) (2). The continuous curves correspond to SAFT-VR predictions and the circles to the experimental data.[72]

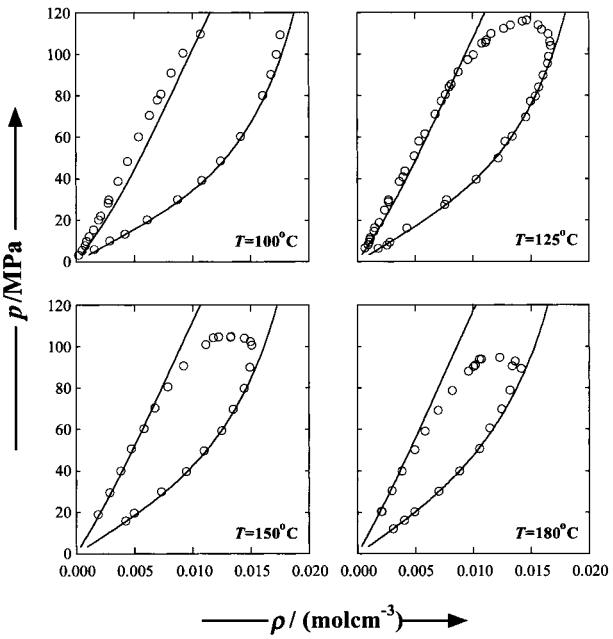

Figure 2. Constant-temperature *pρ* slices of the phase diagram for methane (1) + *n*-hexatriacontane ($C_{36}H_{74}$) (2). The continuous curves correspond to SAFT-VR predictions and the circles to the experimental data.[72]

parameters for the alkane mixtures as the approach accounts explicitly for the molecular size through the parameter *m* and the segment−segment interactions are of the same nature in the alkane and polyethylene components. However, we also examine the adsorption of an unsaturated short-chain alkane (ethene) in LPDE. As could be expected, in this case the unlike intermolecular parameters need to be readjusted. The optimized intermolecular parameters for ethene are shown in Table 1.

As an extension of earlier work,[58] we concentrate here on mixtures of short- and long-chain (up to polymer-like) alkane molecules. The first system we have studied is the methane (1) + *n*-hexatriacontane (2) binary mixture. Four constant-temperature *px* slices of the phase diagram in which the SAFT-VR predictions are compared with the experimental data of Marteau et al.[72] are shown in Figure 1. The SAFT-VR approach gives a very good description of the experimental phase behavior, especially in the low-pressure region. As expected for an analytical equation of state, the critical point is overestimated;[71] better agreement in this region can be obtained by rescaling the model parameters to the critical points of the pure components in a mixture (see, for example, refs 55−57), although this is always at the expense of poorer agreement at lower temperatures and pressures. Together with the *px* slices, we also compared the SAFT-VR predictions with experimental data for constant-temperature pressure−density *pρ* diagrams (Figure 2). Excellent agreement is again obtained.

Following the study of methane + *n*-hexatriacontane, it is possible to examine in the same way the vapor−liquid adsorption equilibrium of a short-chain hydrocarbon molecule in low-density polyethylene (LDPE). In the SAFT approach, the extension to longer molecules is straightforward. As mentioned earlier, a relation between the number of carbons in the alkane chain (or the molecular weight of a polymer) and the number of segments *m* forming the corresponding chain model molecules is used. As the size of the heavier molecule increases, its vapor pressure decreases. As a result, the

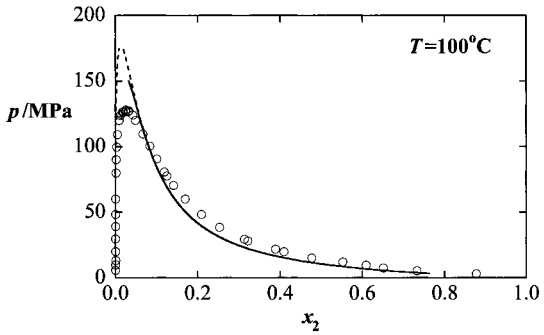

Figure 3. Constant-temperature *px* slice of the phase diagram for methane (1) + *n*-hexatriacontane ($C_{36}H_{74}$) (2) at $T = 100$ °C. The dashed curves correspond to the original SAFT-VR prediction and the solid line to a calculation restricting the polymer to the liquid phase. The circles correspond to the experimental data.[72]

vapor phase contains practically no polymer (i.e., only the short-chain alkane molecule is found in the vapor phase). To illustrate this point, we compare (in Figure 3) our previous calculation of the phase behavior of methane (1) + *n*-hexatriacontane (2) with hexatriacontane in both phases (Figure 1) with the result of a calculation in which *n*-hexatriacontane is restricted to the liquid phase. As can be seen from Figure 3, the calculated phase boundaries of the liquid are almost identical in both cases for this mixture; in the case of heavier polymer molecules, the slight difference observed will become insignificant. In Figure 4, the adsorption equilibrium of *n*-pentane (1) in a melt of LDPE of molecular weight 76 000 g/mol (2) is examined. The SAFT-VR calculations are compared with the experimental data of Surana et al.[73] at $T = 150$ °C. The SAFT-VR approach clearly provides an excellent description of the phase behavior of the system at this temperature. It is especially encouraging to note that no unlike adjustable parameters were used in these theoretical predictions. Note, however, that because we only examine vapor−liquid equilibria in this work, at

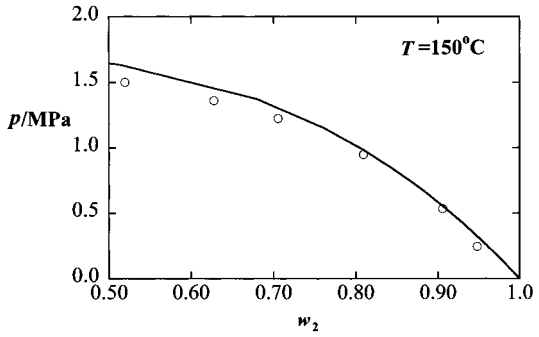

Figure 4. Constant-temperature *pw* slice of the phase diagram for pentane (1) + LDPE (M_w = 76 000) (2) at T = 150 °C. The continuous curves correspond to the SAFT-VR prediction and the circles to the experimental data of Surana et al.[73]

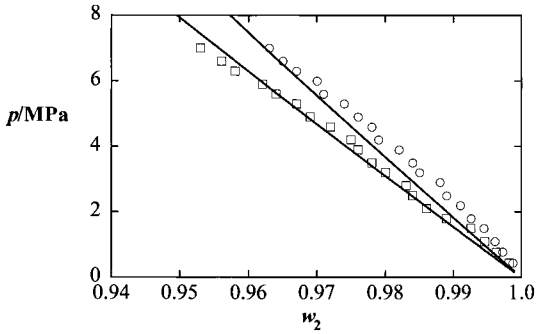

Figure 5. Constant-temperature *pw* slices of the phase diagram for ethene (1) + LDPE (M_w = 248 700) (2) at T = 126 and T = 155 °C. The continuous curves correspond to the SAFT-VR predictions and the symbols to the data of Hao et al.[74] (squares for 126 °C and circles for 155 °C).

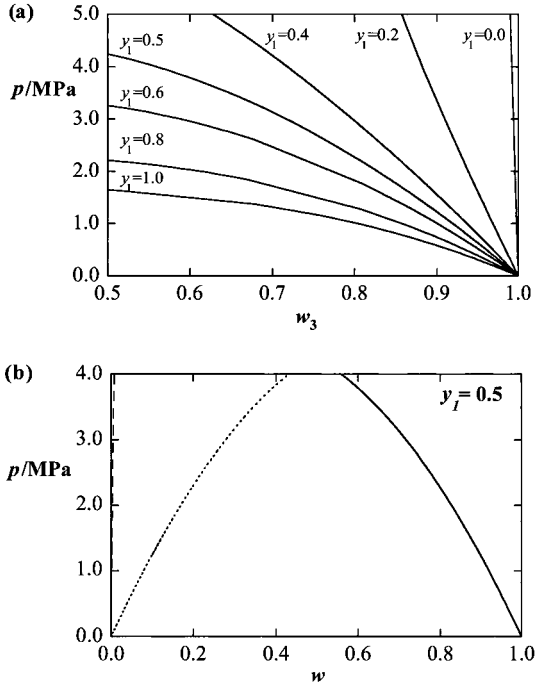

Figure 6. (a) Constant-temperature *pw* slices of the phase diagram for pentane (1) + methane (2) + LDPE (M_w = 76 000) (3) at T = 150 °C. The curves correspond to calculated weight fractions of the polymer w_3 in the liquid phase for different compositions y of the gas phase. (b) Weight fractions w of each component in the liquid phase for a 50:50 gas composition of the two short-chain alkanes in the pentane (1) + methane (2) + LDPE (M_w = 76 000) (3) ternary system at T = 150 °C. The dotted curve corresponds to pentane, the dashed curve to methane, and the continuous curve to LDPE.

T = 150 °C, one should not extend the current calculations to polymer weight fractions of less than 0.5 for this system (the corresponding vapor pressure here is p = 1.6 MPa); liquid−liquid separation is expected beyond this point. As mentioned in the Introduction, liquid−liquid phase separation occurs in mixtures of short and long alkanes a result of the size difference between the two components. At a constant temperature, the upper pressure limit of the immiscibility corresponds to a critical point, while the lower pressure limit is a point of three-phase coexistence (i.e., where the liquid−liquid region meets the vapor−liquid region, see Figures 3 and 5 of ref 56). This three-phase coexistence typically occurs at pressures just below the pure vapor pressure of the more volatile component (the short alkane), and in the case of pentane, the vapor pressure at T = 150 °C is p = 1.615 MPa. Similarly, we examine the adsorption vapor−liquid equilibrium of ethene (1) in a LDPE of molecular weight 248 700 g/mol (2) (see Figure 5). Good agreement between the SAFT-VR prediction and the experimental data is again obtained for the two constant-temperature *pw* slices studied, although for the adsorption of ethene, we have used an adjustable binary interaction parameter for the unlike attractive dispersion interaction [ξ = 0.94, where $\alpha_{12} = \xi(\alpha_{11}\ \alpha_{22})^{1/2}$]; ξ was obtained by comparison with the experimental vapor−liquid equilibria data at T = 155 °C.[74] It is not surprising that an adjustable parameter is required for this system as the interactions between unsaturated and saturated alkanes are expected to be different than those between saturated alkanes.

Additionally, we have carried out a purely predictive theoretical study of the coadsorption of two short-chain alkanes in LDPE. We consider the different fractionation of the short-chain hydrocarbons in the vapor (pure short-chain alkane) and liquid (short-chain alkane and polymer) phases. For equal compositions of the gas phase y, very different adsorption ratios are observed depending on the relative nature of the comonomers. The adsorption for a ternary mixture of pentane (1) + methane (2) + LPDE 76 000 g/mol (3) at T = 150 °C is studied in Figure 6. The pressure over the polymer phase as a function of polymer composition for different gas composition ratios of the comonomers is shown in Figure 6a. For $y_1 = 0$ ($y_2 = 1.0$, $y_3 = 0$), the gas phase is pure methane, and the highest pressures are observed. When the proportion of pentane in the gas phase increases, the equilibrium pressure decreases, as expected, until, for $y_1 = 1.0$ ($y_2 = 0$, $y_3 = 0$), an adsorption curve equivalent to that shown in Figure 4 for the binary system of pentane + LDPE is seen. The decrease in vapor pressure for the higher ratios of pentane is a consequence of the lower volatility of pentane compared to methane. From this representation of the phase behavior, however, no information is obtained for the amount of short-chain hydrocarbon adsorbed in the polymer liquid phase. In Figure 6b, we examine the weight fractions of each component in the liquid phase w for a 50:50 gas composition of the two short-chain *n*-alkanes. It can be seen from the figure that, as the pressure increases, significantly more pentane is adsorbed than methane; given the higher vapor pressure of methane, it is mostly found in the gas phase. We have carried out a similar coadsorption study for a mixture of pentane (1) + butane (2) + LDPE 76 000 g/mol (3) at the same constant temperature (Figure 7). In terms of the pressure/composition *pw* diagram, for fixed gas-phase compositions, a phase diagram equivalent to the

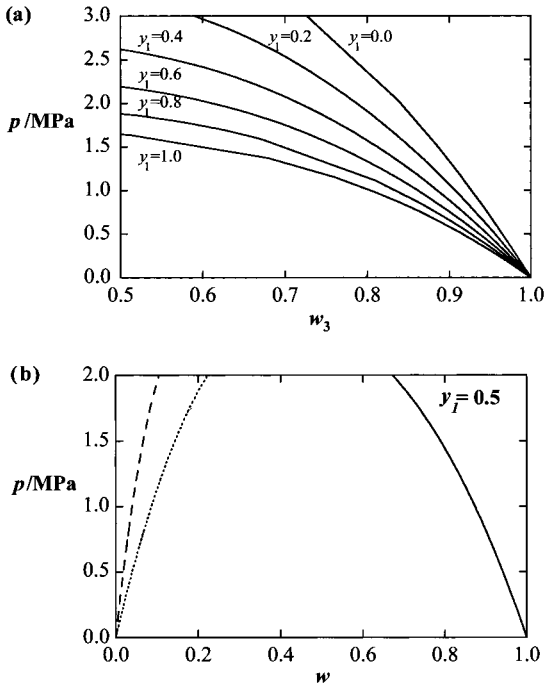

Figure 7. (a) Constant-temperature pw slices of the phase diagram for pentane (1) + butane (2) + LDPE (M_w = 76 000) (3) phase diagram at T = 150 °C. The curves correspond to the calculated polymer weight fractions w_3 in the liquid phase for different compositions y of the gas phase. (b) Weight fractions w of each component in the liquid phase for a 50:50 gas composition of the two short-chain alkanes in the pentane (1) + methane (2) + LDPE (M_w = 76 000) (3) ternary system at T = 150 °C. The dotted curve corresponds to pentane, the dashed curve to butane, and the continuous curve to LDPE.

previous one is obtained; the vapor pressure is seen to decrease as the amount of pentane in the gas phase increases. In terms of the amount of short-chain alkane molecules adsorbed in the polymer liquid phase, however, it can clearly be seen that the two alkanes (butane and pentane) are more evenly adsorbed in this case, as expected given the similar vapor pressures of pentane and butane for a given temperature. For example, at a pressure of 2 MPa, the ratio of the weight fractions of the short-chain alkanes is $w_1/w_2 = 0.001$ in the mixture of pentane (1) + methane (2) + LDPE 76 000 g/mol (3), whereas at the same pressure in the mixture of pentane (1) + butane (2) + LDPE 76 000 g/mol (3), the ratio of the weight fractions is $w_1/w_2 = 0.47$. We have not been able to find suitable experimental data for comparison, although in a polymerization process, a mixture of short-chain alkanes will be in equilibrium with the polymer. The phase diagrams of the multicomponent systems are thus of crucial interest.

In conclusion, we have used the SAFT-VR approach to study the phase behavior of short and long hydrocarbons. Using simple linear relations developed from the intermolecular potential parameters for the *n*-alkanes from methane to hexatriacontane, we are able to determine parameters for LPDE chains of a given molecular weight. We have examined the adsorption of a number of monomers in LDPE and find excellent agreement with experimental data. In this work, we have concentrated on the vapor−liquid adsorption equilibria of these systems; soon, we plan to examine the complete phase diagrams, including also the liquid−liquid equilibria (cloud curves) commonly found in polymer systems.

Acknowledgment

C. Mc. thanks Sheffield University for the award of a UGC Scholarship, A. G. thanks the EPSRC for the award of an Advanced Fellowship. M. N. G. thanks BP−Amoco for funding a Research Fellowship. We also acknowledge support from the European Commission, the Royal Society, and the JREI (GR/M94427) and ROPA (GR/N20317) Initiatives of the EPSRC for the provision of computer hardware.

Literature Cited

(1) Scott, R. L.; van Konynenburg, P. H. *Discuss. Faraday Soc.* **1970**, 49.

(2) Smith, B. D.; Srivastava, R. *Thermodynamic Data for Pure Compounds*; Elsevier: London, 1986.

(3) Younglove, B. A.; Ely, J. F. Thermo-Physical Properties of Fluids. 2. Methane, Ethane, Propane, Isobutane, and Normal Butane. *J. Phys. Chem. Ref. Data* **1987**, *16*, 577−798.

(4) Reid, R. C.; Prausnitz, J. M.; Poling, B. E. *The Properties of Gases and Liquids*, 4th ed.; McGraw-Hill: New York, 1987.

(5) Schaerer, A. A.; Busso, C. J.; Smith, A. E.; Skinner, L. B. Properties of pure normal alkanes in the C_{17} to C_{36} range. *J. Am. Chem. Soc.* **1955**, *77*, 2017−2019.

(6) Morecroft, D. W. Vapour pressures of some high molecular weight hydrocarbons. *J. Chem. Eng. Data* **1964**, *9*, 488−490.

(7) Anselme, M. J.; Gude, M.; Teja, A. S. The Critical Temperatures and Densities of the Normal Alkanes from Pentane to Octadecane. *Fluid Phase Equilib.* **1990**, *57*, 317−326.

(8) Bokis, C. P.; Orbey, H.; Chen, C. C. Properly model polymer processes. *Chem. Eng. Prog.* **1999**, *95*, 39−52.

(9) Danner, R. P.; High, M. S. *Handbook of Polymer Solution Dynamics*; American Institute of Chemical Engineers: New York, 1993.

(10) Bokis, C. P.; Chen, C. C.; Orbey, H. A segment contribution method for the vapor pressure of tall-oil chemicals. *Fluid Phase Equilib.* **1999**, *155*, 193−203.

(11) Prausnitz, J. M.; Lichtenthaler, R. N.; Gomes de Azecedo, E. *Molecular Thermodynamics of Fluid-Phase Equilibria*, 2nd ed.; Prentice Hall: Englewood Cliffs, NJ, 1986.

(12) Huggins, M. L. Thermodynamics of polymer solutions. *J. Chem. Phys.* **1942**, *10*, 51−61.

(13) Chen, C. A Segment-Based Local Composition Model for the Gibbs Energy of Polymer Solutions. *Fluid Phase Equilib.* **1993**, *83*, 301−312.

(14) Oishi, T.; Prausnitz, J. M. Estimation of Solvent Activities in Polymer Solutions Using a Group-Contribution Methodology. *Ind. Eng. Chem. Process Des. Dev.* **1978**, *17*, 333−339.

(15) Sanchez, I. C.; Lacombe, R. H. Elementary Molecular Theory of Classical Fluids−Pure Fluids. *J. Phys. Chem.* **1976**, *80*, 2352−2362.

(16) Lacombe, R. H.; Sanchez, I. C. Statistical Thermodynamics of Fluid Mixtures. *J. Phys. Chem.* **1976**, *80*, 2569−2580.

(17) Sanchez, I. C.; Lacombe, R. H. Statistical Thermodynamics of Polymer Solutions. *Macromolecules* **1978**, *11*, 1145−1156.

(18) Fischer, K.; Gmehling, J. Further development, status and results of the PSRK method for the prediction of vapor−liquid equilibria and gas solubilities. *Fluid Phase Equilib.* **1996**, *121*, 185−206.

(19) Chapman, W. G.; Gubbins, K. E.; Jackson, G.; Radosz, M. SAFT−Equation-of-State Solution Model for Associating Fluids. *Fluid Phase Equilib.* **1989**, *52*, 31−38.

(20) Chapman, W. G.; Gubbins, K. E.; Jackson, G.; Radosz, M. New Reference Equation of State for Associating Liquids. *Ind. Eng. Chem. Res.* **1990**, *29*, 1709−1721.

(21) Orbey, H.; Chen, C. C.; Bokis, C. P. An extension of cubic equations of state to vapor−liquid equilibria in polymer−solvent mixtures. *Fluid Phase Equilib.* **1998**, *145*, 169−192.

(22) Orbey, H.; Bokis, C. P.; Chen, C. C. Polymer−solvent vapor−liquid equilibrium: Equations of state versus activity coefficient models. *Ind. Eng. Chem. Res.* **1998**, *37*, 1567−1573.

(23) Wertheim, M. S. Fluids with Highly Directional Attractive Forces. 2. Thermodynamic Perturbation Theory and Integral Equations. *J. Stat. Phys.* **1984**, *35*, 35−47.

(24) Wertheim, M. S. Fluids with Highly Directional Attractive Forces. 1. Statistical Thermodynamics. *J. Stat. Phys.* **1984**, *35*, 19−34.

(25) Wertheim, M. S. Fluids with Highly Directional Attractive Forces. 3. Multiple Attraction Sites. *J. Stat. Phys.* **1986**, *42*, 459−476.

(26) Wertheim, M. S. Fluids with Highly Directional Attractive Forces. 4. Equilibrium Polymerization. *J. Stat. Phys.* **1986**, *42*, 477−492.

(27) Huang, S. H.; Radosz, M. Equation of State for Small, Large, Polydisperse, and Associating Molecules. *Ind. Eng. Chem. Res.* **1990**, *29*, 2284−2294.

(28) Huang, S. H.; Radosz, M. Equation of State for Small, Large, Polydisperse, and Associating Molecules−Extension to Fluid Mixtures. *Ind. Eng. Chem. Res.* **1991**, *30*, 1994−2005.

(29) Huang, S. H.; Radosz, M. Equation of State for Small, Large, Polydisperse, and Associating Molecules−Extension to Fluid Mixtures. *Ind. Eng. Chem. Res.* **1993**, *32*, 762−762.

(30) Wu, C. S.; Chen, Y. P. Calculation of Vapor−Liquid Equilibria of Polymer Solutions Using the SAFT Equation of State. *Fluid Phase Equilib.* **1994**, *100*, 103−119.

(31) Chapman, W. G. Prediction of the Thermodynamic Properties of Associating Lennard-Jones Fluids−Theory and Simulation. *J. Chem. Phys.* **1990**, *93*, 4299−4304.

(32) Johnson, J. K.; Gubbins, K. E. Phase Equilibria for Associating Lennard-Jones Fluids From Theory and Simulation. *Mol. Phys.* **1992**, *77*, 1033−1053.

(33) Ghonasgi, D.; Chapman, W. G. Theory and Simulation for Associating Chain Fluids. *Mol. Phys.* **1993**, *80*, 161−176.

(34) Ghonasgi, D.; Llanorestrepo, M.; Chapman, W. G. Henry Law Constant for Diatomic and Polyatomic Lennard-Jones Molecules. *J. Chem. Phys.* **1993**, *98*, 5662−5667.

(35) Ghonasgi, D.; Chapman, W. G. Prediction of the Properties of Model Polymer Solutions and Blends. *AIChE J.* **1994**, *40*, 878−887.

(36) Johnson, J. K.; Muller, E. A.; Gubbins, K. E. Equation of State for Lennard-Jones Chains. *J. Phys. Chem.* **1994**, *98*, 6413−6419.

(37) Banaszak, M.; Chiew, Y. C.; Olenick, R.; Radosz, M. Thermodynamic Perturbation Theory−Lennard-Jones Chains. *J. Chem. Phys.* **1994**, *100*, 3803−3807.

(38) Blas, F. J.; Vega, L. F. Thermodynamic behaviour of homonuclear and heteronuclear Lennard-Jones chains with association sites from simulation and theory. *Mol. Phys.* **1997**, *92*, 135−150.

(39) Blas, F. J.; Vega, L. F. Critical behavior and partial miscibility phenomena in binary mixtures of hydrocarbons by the statistical associating fluid theory. *J. Chem. Phys.* **1998**, *109*, 7405−7413.

(40) Vega, L. F.; Blas, F. J. Tricritical phenomena in chain-like mixtures from a molecular-based equation of state. *Fluid Phase Equilib.* **2000**, *171*, 91−104.

(41) Davies, L. A.; Gil-Villegas, A.; Jackson, G. Describing the properties of chains of segments interacting via soft-core potentials of variable range with the SAFT-VR approach. *International J. Thermophysics* **1998**, *19*, 675−686.

(42) Jackson, G.; Chapman, W. G.; Gubbins, K. E. Phase Equilibria of Associating Fluids−Spherical Molecules with Multiple Bonding Sites. *Mol. Phys.* **1988**, *65*, 1−31.

(43) Chapman, W. G.; Jackson, G.; Gubbins, K. E. Phase Equilibria of Associating Fluids Chain Molecules with Multiple Bonding Sites. *Mol. Phys.* **1988**, *65*, 1057−1079.

(44) Galindo, A.; Whitehead, P. J.; Jackson, G.; Burgess, A. N. Predicting the phase equilibria of mixtures of hydrogen fluoride with water, difluoromethane (HFC-32), and 1,1,1,2-tetrafluoroethane (HFC-134a) using a simplified SAFT approach. *J. Phys. Chem. B* **1997**, *101*, 2082−2091.

(45) Galindo, A.; Whitehead, P. J.; Jackson, G.; Burgess, A. N. Predicting the high-pressure phase equilibria of water plus *n*-alkanes using a simplified SAFT theory with transferable intermolecular interaction parameters. *J. Phys. Chem.* **1996**, *100*, 6781−6792.

(46) Garcia-Lisbona, M. N.; Galindo, A.; Jackson, G.; Burgess, A. N. Predicting the high-pressure phase equilibria of binary aqueous solutions of 1-butanol, *n*-butoxyethanol and *n*-decylpentaoxyethylene ether (C10E5) using the SAFT-HS approach. *Mol. Phys.* **1998**, *93*, 57−71.

(47) Garcia-Lisbona, M. N.; Galindo, A.; Jackson, G.; Burgess, A. N. An examination of the cloud curves of liquid−liquid immiscibility in aqueous solutions of alkyl polyoxyethylene surfactants using the SAFT-HS approach with transferable parameters. *J. Am. Chem. Soc.* **1998**, *120*, 4191−4199.

(48) Gil-Villegas, A.; Galindo, A.; Whitehead, P. J.; Mills, S. J.; Jackson, G.; Burgess, A. N. Statistical associating fluid theory for chain molecules with attractive potentials of variable range. *J. Chem. Phys.* **1997**, *106*, 4168−4186.

(49) Galindo, A.; Davies, L. A.; Gil-Villegas, A.; Jackson, G. The thermodynamics of mixtures and the corresponding mixing rules in the SAFT-VR approach for potentials of variable range. *Mol. Phys.* **1998**, *93*, 241−252.

(50) Adidharma, H.; Radosz, M. Prototype of an engineering equation of state for heterosegmented polymers. *Ind. Eng. Chem. Res.* **1998**, *37*, 4453−4462.

(51) Adidharma, H.; Radosz, M. Square-well SAFT equation of state for homopolymeric and heteropolymeric fluids. *Fluid Phase Equilib.* **1999**, *160*, 165−174.

(52) Chan, A. K. C.; Adidharma, H.; Radosz, M. Fluid−liquid transitions of poly(ethylene-*co*-octene-1) in supercritical ethylene solutions. *Ind. Eng. Chem. Res.* **2000**, *39*, 4370−4375.

(53) Chan, A. K. C.; Russo, P. S.; Radosz, M. Fluid−liquid equilibria in poly(ethylene-*co*-hexene-1) plus propane: A light-scattering probe of cloud-point pressure and critical polymer concentration. *Fluid Phase Equilib.* **2000**, *173*, 149−158.

(54) Chan, K. C.; Adidharma, H.; Radosz, M. Fluid−liquid and fluid−solid transitions of poly(ethylene-*co*- octene-1) in sub- and supercritical propane solutions. *Ind. Eng. Chem. Res.* **2000**, *39*, 3069−3075.

(55) McCabe, C.; Galindo, A.; Gil-Villegas, A.; Jackson, G. Predicting the high-pressure phase equilibria of binary mixtures of *n*-alkanes using the SAFT-VR approach. *Int. J. Thermophys.* **1998**, *19*, 1511−1522.

(56) McCabe, C.; Gil-Villegas, A.; Jackson, G. Predicting the high-pressure phase equilibria of methane plus *n*-hexane using the SAFT-VR approach. *J. Phys. Chem. B* **1998**, *102*, 4183−4188.

(57) McCabe, C.; Galindo, A.; Gil-Villegas, A.; Jackson, G. Predicting the high-pressure phase equilibria of binary mixtures of perfluoro-*n*-alkanes plus *n*-alkanes using the SAFT-VR approach. *J. Phys. Chem. B* **1998**, *102*, 8060−8069.

(58) McCabe, C.; Jackson, G. SAFT-VR modelling of the phase equilibrium of long-chain *n*-alkanes. *Phys. Chem. Chem. Phys.* **1999**, *1*, 2057−2064.

(59) Galindo, A.; Gil-Villegas, A.; Whitehead, P. J.; Jackson, G.; Burgess, A. N. Prediction of phase equilibria for refrigerant mixtures of difluoromethane (HFC-32), 1,1,1,2-tetrafluoroethane (HFC-134a), and pentafluoroethane (HFC-125a) using SAFT-VR. *J. Phys. Chem. B* **1998**, *102*, 7632−7639.

(60) Filipe, E. J. M.; de Azevedo, E.; Martins, L. F. G.; Soares, V. A. M.; Calado, J. C. G.; McCabe, C.; Jackson, G. Thermodynamics of Liquid Mixtures of Xenon with Alkanes: (Xenon + Ethane) and (Xenon + Propane). *J. Phys. Chem. B* **2000**, *104*, 1315−1321.

(61) Filipe, E. J. M.; Martins, L. F. G.; Calado, J. C. G.; McCabe, C.; Jackson, G. Thermodynamics of Liquid Mixtures of Xenon with Alkanes: (Xenon + *n*-Butane) and (Xenon + Isobutane). *J. Phys. Chem. B* **2000**, *104*, 1322−1325.

(62) Fu, Y. H.; Sandler, S. I. A Simplified SAFT Equation of State for Associating Compounds and Mixtures. *Ind. Eng. Chem. Res.* **1995**, *34*, 1897−1909.

(63) Blas, F. J.; Vega, L. F. Prediction of Binary and Ternary Diagrams Using the Statistical Associating Fluid Theory (SAFT) Equation of State. *Ind. Eng. Chem. Res.* **1998**, *37*, 660−674.

(64) Siepmann, J. I.; Karaborni, S.; Smit, B. Simulating the critical behaviour of complex fluids. *Nature* **1993**, *365*, 330.

(65) Smit, B.; Karaborni, S.; Siepmann, J. I. Computer Simulations of the Vapor−Liquid Phase Equilibria of *n*-Alkanes. *J. Chem. Phys.* **1995**, *102*, 2126.

(66) Leonard, P. J.; Henderson, D.; Barker, J. A. Perturbation Theory and Liquid Mixtures. *Trans. Faraday Soc.* **1970**, *66*, 2439.

(67) Boublik, T. Hard-Sphere Equation of State. *J. Chem. Phys.* **1970**, *53*, 471.

(68) Mansoori, G. A.; Carnahan, N. F.; Starling, K. E.; Leland, T. W. Equilibrium Thermodynamic Properties of Mixture of Hard Spheres. *J. Chem. Phys.* **1971**, *54*, 1523.

(69) Jackson, G.; Gubbins, K. E. Mixtures of Associating Spherical and Chain Molecules. *Pure Appl. Chem.* **1989**, *61*, 1021−1026.

(70) Press: W. H.; Teukolsky, S. A.; Vetterling, W. T.; Flannery, B. P. *Numerical Recipes in FORTRAN*, 1st ed.; Cambridge University Press: New York, 1986.

(71) Rowlinson, J. S.; Swinton, F. L. *Liquids and Liquid Mixtures*, 3rd ed.; Butterworth Scientific: London, 1982.

(72) Marteau, P.; Tobaly, P.; Ruffier-Meray, V.; de Hemptinne, J. C. High-pressure phase diagrams of methane plus squalane and methane plus hexatriacontane mixtures. *J. Chem. Eng. Data* **1998**, *43*, 362−366.

(73) Surana, R. K.; Danner, R. P.; de Hann, A. B.; Beckers, N. New technique to measure high-pressure and high-temperature polymer−solvent vapour−liquid equilibrium. *Fluid Phase Equilib.* **1997**, *139*, 361−370.

(74) *Polymer Solution Data Collection*; Hao, W., Elbro, H. S., Alessi, P., Eds.; DECHEMA: Frankfurt, Germany, 1992; Vol. XIV, Part 1.

Received for review February 12, 2001
Revised manuscript received June 15, 2001
Accepted June 20, 2001

IE0101386